Published in final edited form as:
Genesis. 2010 May ; 48(5): 328–342. doi:10.1002/dvg.20620.

Ehd4 is required to attain normal pre-pubertal testis size but dispensable for fertility in male mice

Manju George[1,#], **Mark A. Rainey**[1,#], **Mayumi Naramura**[1,#,*], **GuoGuang Ying**[2,#], **Don W. Harms**[3], **Martha H. Vitaterna**[4], **Lynn Doglio**[5], **Susan E. Crawford**[6], **Rex A. Hess**[7], **Vimla Band**[1,8,9,#], and **Hamid Band**[1,8,9,#,*]

[1]Eppley Institute for Research in Cancer and Allied Diseases, University of Nebraska Medical Center, Omaha, Nebraska, USA

[2]Laboratory of Molecular Oncology, Tianjin Medical University Cancer Institute and Hospital, Tianjin, China

[3]Mouse Genome Engineering Core facility, Department of Genetics, Cell Biology and Anatomy, and College of Medicine, University of Nebraska Medical Center, Omaha, Nebraska, USA

[4]Department of Neurobiology and Physiology, Northwestern University, Evanston, IL 60208

[5]Department of Medicine Northwestern University Feinberg School of Medicine, Chicago, Illinois, USA

[6]Department of Pathology, Northwestern University Feinberg School of Medicine, Chicago, Illinois, USA

[7]Department of Veterinary Bioscience, University of Illinois at Urbana-Champaign, Urbana, Illinois, USA

[8]Department of Genetics, Cell Biology and Anatomy, and College of Medicine, University of Nebraska Medical Center, Omaha, Nebraska, USA

[9]Department of Biochemistry and Molecular Biology, College of Medicine, University of Nebraska Medical Center, Omaha, Nebraska, USA

Abstract

The four highly homologous members of the C-terminal EH domain-containing (EHD) protein family (EHD1-4) regulates endocytic recycling. To delineate the role of EHD4 in normal physiology and development, mice with a conditional knockout of the *Ehd4* gene were generated. PCR of genomic DNA and Western blotting of organ lysates from $Ehd4^{-/-}$ mice confirmed EHD4 deletion. $Ehd4^{-/-}$ mice were viable and born at expected Mendelian ratios; however, males showed a 50% reduction in testis weight, obvious from postnatal day 31. An early (day 10) increase in germ cell proliferation and apoptosis and a later increase in apoptosis (day 31) were seen in the $Ehd4^{-/-}$ testis. Other defects included a progressive reduction in seminiferous tubule diameter, dysregulation of seminiferous epithelium and head abnormalities in elongated spermatids. As a consequence, lower sperm counts and reduced fertility were observed in $Ehd4^{-/-}$ males. Interestingly, EHD protein expression was seen to be temporally regulated in the testis and

Correspondence and requests for materials should be addressed to Dr. Hamid Band (hband@unmc.edu) or Dr. Mayumi Naramura (mnaramura@unmc.edu).. *Corresponding authors: Hamid Band, phone: (402)-559-8572, fax: (402)-559-2823, hband@unmc.edu and Mayumi Naramura, phone: (402)-559-8573, fax: (402)-559-2823, mnaramura@unmc.edu. .
#This work was initiated and partially completed while the indicated authors were at: Department of Medicine, Evanston Northwestern Healthcare Research Institute, Northwestern University Feinberg School of Medicine, Evanston, IL, USA

The authors declare no potential conflicts of interest.

levels peaked between days 10 and 15. In the adult testis, EHD4 was highly expressed in primary spermatocytes and EHD4 deletion altered the levels of other EHD proteins in an age-dependent manner. We conclude that high levels of EHD1in the adult *Ehd4*$^{-/-}$ testis functionally compensate for lack of EHD4 and prevents the development of severe fertility defects. Our results suggest a role for EHD4 in the proper development of post-mitotic and post-meiotic germ cells and implicate EHD protein-mediated endocytic recycling as an important process in germ cell development and testis function.

Introduction

Endocytic recycling, a process that returns internalized membrane and membrane-associated proteins back to the cell surface is essential for various cellular functions such as migration, cell division and regulation of signaling (Maxfield and McGraw, 2004). Recently, a highly conserved four-member family of C-terminal Eps15 homology-domain containing (EHD) proteins (EHD1-4) has been shown to regulate various aspects of endocytic recycling (Grant and Caplan, 2008). EHD proteins are characterized by an EH domain at the C-terminus, a nucleotide binding P-loop near the N-terminus and a central coiled-coiled region. The EH domain mediates protein–protein interactions by binding to the Asn-Pro-Phe (NPF) tri-peptide motif present in interacting proteins and also facilitates membrane binding through association with membrane phospholipids (Naslavsky, *et al.*, 2007a; Blume, *et al.*, 2007). The P-loop binds and hydrolyzes ATP at a very slow rate *in vitro* (Lee, *et al.*, 2005). Exogenously expressed EHD proteins associate with each other as homo- or hetero-oligomers (Braun, *et al.*, 2005; George, *et al.*, 2007), and this observation was confirmed with endogenous EHD1 and EHD4 proteins (Sharma, *et al.*, 2008). A point mutation in the coiled-coiled region of EHD1 (V203P) decreases oligomerization with itself and EHD3, indicating that this region is involved in interaction of EHD proteins with each other. A large number of EHD interacting proteins have been identified. Many of these appear to regulate trafficking of a number of cell-surface receptors (Grant and Caplan, 2008).

EHD2 regulates insulin mediated GLUT4 trafficking to the cell surface (Guilherme, *et al.*, 2004). Structural studies of EHD2 have suggested a dynamin-like role for EHD2 in membrane scission (Daumke, *et al.*, 2007). EHD2 is also involved in myoblast fusion and interacts with myoferlin (Doherty, *et al.*, 2008). EHD3 interacts with EHD1 and functions in the early endosome to facilitate transfer of cargo from the early endosomes to recycling endosomes (Naslavsky, *et al.*, 2006) as well as from early endosomes to the Golgi (Naslavsky, *et al.*, 2009).

EHD4 was initially described as a protein expressed in the extracellular matrix (Kuo, *et al.*, 2001) but has subsequently been shown to be a cytosolic and endosomal vesicle-associated protein. It functions in regulating the exit of endocytic cargo from the early endosomes toward the recycling endosomes (George, *et al.*, 2007) and late endosomes (Sharma, *et al.*, 2008). EHD4 is induced upon NGF stimulation in PC12 cells and regulates retrograde endosomal trafficking of NGF/TrkA (Shao, *et al.*, 2002; Valdez, *et al.*, 2005). Recently, it has been shown to be involved along with Rac1 and phosphatidyl inositol 3-kinase in a novel bulk endocytic pathway for membrane retrieval in neuronal growth cones (Bonanomi, *et al.*, 2008).

A previous study (George, *et al.*, 2007) comparing all EHD proteins side-by-side in a *C. elegans* complementation assay as well as co-localization and transferrin recycling assays in HeLa cells indicated that EHD proteins have distinct as well as overlapping functions. Another study, (Blume, *et al.*, 2007) compared EHD proteins with respect to tissue distribution, intracellular localization and lipid binding properties; this study concluded that

different EHD proteins may be restricted to different tissues and intracellular compartments or organelles and may perform specific functions. However, little is known about the role of EHD proteins in normal mammalian physiology and development. A published report on EHD1 knockout mice described the lack of phenotypes in these mice apart from a minor delay in transferrin recycling in isolated mouse embryonic fibroblasts (MEFs) (Rapaport, *et al.*, 2006). MEFs derived from these EHD1 knockout mice also exhibited defects in β1 integrin trafficking, cell spreading and migration (Jovic, *et al.*, 2007) as well as cholesterol homeostasis (Naslavsky, *et al.*, 2007b). No information is available on the physiological role of other mammalian EHD proteins.

To understand the role of EHD4 in normal mouse physiology and development, mice with targeted deletion of *Ehd4* were engineered. The main observable phenotype in *Ehd4*$^{-/-}$ mice was a substantial reduction in testicular size, sperm count and slight reduction in fertility. Our results suggest that mammalian EHD4 functions redundantly with other family members in most organs, but is required for efficient survival of germ cells and attainment of normal pre-pubertal testicular size in mice.

Results

Generation of *Ehd4*$^{-/-}$ mice

In an effort to create EHD4 knockout mice, we targeted the first exon of *Ehd4* such that targeted animals would not express EHD4 (Fig. 1a). Three correctly-targeted ES cell clones were used for blastocyst injections to produce chimeric mice; one of these achieved germline transmission of the targeted *Ehd4* allele. We generated *Ehd4* homozygous floxed as well as deleted mice as described in Methods. PCR was used for genotyping (Fig. 1b). Intercrosses among heterozygous (*Ehd4*$^{+/-}$) mice produced *Ehd4*$^{+/+}$, *Ehd4*$^{+/-}$ and *Ehd4*$^{-/-}$ mice at the expected Mendelian ratios (Table 1).

Absence of EHD4 expression in *Ehd4*$^{-/-}$ mice

To confirm the lack of EHD4 expression in *Ehd4*$^{-/-}$ mice, lysates of various organs from *Ehd4*$^{+/+}$, E*hd4*$^{+/-}$ and *Ehd4*$^{-/-}$ mice were analyzed using Western blotting with previously characterized antibodies. The antibody used to detect EHD4 was raised against a peptide in the EH domain and has been previously shown to be specific to EHD4 (George, *et al.*, 2007). Specificity of the EHD4 antibody was further confirmed by immunoprecipitation of endogenous EHD4 from U2OS cell lysates which express all EHD proteins; the antibody specifically immunoprecipitated EHD4, but not other EHD proteins (Supplementary Material Fig.1). Using this EHD4 antibody, a 64-kDa EHD4 band was evident in lysates of all wild type tissues tested (Fig. 2) except for liver where a band was observed only after longer exposure (data not shown). No EHD4 was detected in the lung, kidney, heart, spleen, brain, liver, thymus or testis of *Ehd4*$^{-/-}$ mice even after long exposures. This is in agreement with the PCR genotyping results for the mice (Fig. 1B). In *Ehd4*$^{+/-}$ mice, EHD4 was seen in the lung, kidney, spleen, brain, thymus and testis, but at levels approximately half that of respective tissues from wild type animals. As *Ehd4*$^{-/-}$ mice harbor deletion of only the first exon, we considered the possibility that internal translation initiation may result in truncated EHD4 proteins. However no smaller EHD4 peptides were observed in *Ehd4*$^{-/-}$ samples even though the anti-EHD4 antibody was raised against the C-terminal EH domain of EHD4 and should be capable of detecting any aberrant EHD4 proteins generated by internal translation initiation. We, therefore, conclude that deletion of the first exon generated a null allele of *Ehd4*. Interestingly, we observed a compensatory increase in the levels of other EHD proteins in some organs: for example, EHD2 levels were increased in *Ehd4*$^{-/-}$ lung and EHD1 levels were increased in *Ehd4*$^{-/-}$ heart.

Ehd4 $^{-/-}$ males exhibit smaller testes

Ehd4$^{-/-}$ mice appeared healthy and their body weights were comparable to their wild type (*Ehd4*$^{+/+}$) littermates (Table 2). None of the *Ehd4*$^{-/-}$ mice exhibited any gross abnormalities when observed up to 15 months of age. Both male and female *Ehd4*$^{-/-}$ mice appeared fertile and gave rise to healthy offspring.

To further characterize the *Ehd4*$^{-/-}$ mice, various organs were collected from male and female *Ehd4*$^{+/+}$ and *Ehd4*$^{-/-}$ mice and tissue sections were analyzed after Hematoxylin and Eosin (H & E) staining. Most organs analyzed from *Ehd4*$^{-/-}$ mice (lung, kidney, heart, spleen, liver, thymus, skin and brain, data not shown) did not display any significant gross or microscopic abnormalities when compared to wild type littermates. However, *Ehd4*$^{-/-}$ males showed a significant reduction in testis size compared to *Ehd4*$^{+/+}$ mice (Fig. 3a, f). In contrast, spleen weights were comparable between *Ehd4*$^{+/+}$ and *Ehd4*$^{-/-}$ mice at all ages (Fig. 3b), suggesting that the difference in testicular size is not a reflection of a general decrease in organ size in *Ehd4*$^{-/-}$ mice. Given the comparable overall body weights of male *Ehd4*$^{+/+}$ and *Ehd4*$^{-/-}$ mice (Table 2, Fig. 3d), the differences in testis weights suggested specific defects. We did not find a significant difference in the size of seminal vesicles between *Ehd4*$^{+/+}$ and *Ehd4*$^{-/-}$ mice (Fig. 3e); as the development of seminal vesicles is primarily regulated by sex hormones, these results suggested a lack of hormonal differences between *Ehd4* $^{+/+}$ and *Ehd4*$^{-/-}$ male mice. To further characterize the small testis phenotype in *Ehd4*$^{-/-}$ mice, testis was collected from day 10 (d10), d20, d31 mice and weights were recorded. The decrease in testis weights was evident in *Ehd4*$^{-/-}$ mice at 10 days of age, was significantly decreased by 20 days, became more pronounced by day 31 (Fig.3c, Supplementary Material Table 1) and remained significant through 12 months of age (last time point analyzed) (Fig. 3a).

Deletion of EHD4 leads to a progressive reduction in seminiferous tubule diameter in the *Ehd4*$^{-/-}$ testis

The dramatic reduction is testis weight in *Ehd4*$^{-/-}$ mice between d10 and d31 suggested that EHD4 may play a critical role in the testis during this period. Testis development is well defined in mice and the sequence of appearance of different spermatogenic cell types in the pre-pubertal mouse testis is known (Bellve, *et al.*, 1977). For example, at d10, apart from Sertoli cells, type A and B spermatogonia, the seminiferous epithelium contains preleptotene and leptotene primary spermatocytes. By d20, late pachytene cells and early round spermatids make their appearance. Spermatozoa begin to appear in the tubule lumen by d35, marking the first wave of spermatogenesis. After the first wave, the spermatogenic cycle continues in adult mice such that the testis contains all stages of germ cells arranged in a highly organized and efficient manner to form cell associations that are tightly regulated (Clermont, 1972). Even though the efficiency of the process is affected by internal and external variables, the cellular associations and temporal regulation is strictly maintained and is characteristic for a species. Therefore, analysis of *Ehd4*$^{+/+}$ and *Ehd4*$^{-/-}$ testes at various time points (d10, d20, d31 and d75) using H&E and PAS (Periodic Acid Schiff reagent) sections was carried out to assess the impact of EHD4 deficiency. Low magnification images of *Ehd4*$^{+/+}$ and *Ehd4*$^{-/-}$ testes at d20, d31 and d75 clearly show that consistent with the reduction in testis sizes, seminiferous tubules of the *Ehd4*$^{-/-}$ mice were smaller at each age in comparison to wild type mice (Fig. 4) and measurement of tubule diameter confirmed this impression (Table 2). Interestingly, the seminiferous tubule diameter in d10 *Ehd4*$^{-/-}$ testis was slightly larger than that of *Ehd4*$^{+/+}$ testis.

Deletion of EHD4 leads to an increase in apoptosis at d10 and d31 in *Ehd4*$^{-/-}$ testis

During post-natal germ cell development, when germ cells first undergo their complex program of differentiation to become mature spermatozoa, apoptosis is essential (Print and

Loveland, 2000). The first wave of spermatogenesis, beginning by post-natal d5 in mice, is accompanied by a wave of apoptosis that peaks 2–3 weeks after birth and is especially prominent in spermatogonia (Rodriguez, *et al.*, 1997). Only 25% of spermatogonial descendents are estimated to reach the preleptotene spermatocyte stage, the remainder being eliminated by apoptosis (Print and Loveland, 2000). Hence, it is possible that the small testis size and reduced seminiferous tubule diameter in *Ehd4*$^{-/-}$ mice at d20 and later might be due to an earlier increase in apoptosis. Consistent with this possibility, PAS stained sections of d10 *Ehd4*$^{-/-}$ testis showed an increase in apoptotic bodies (Fig. 5h, panel b). To verify the potential increase in apoptosis in *Ehd4*$^{-/-}$ testis, a TUNEL assay was performed on d10, d20 and d31 testis sections. At d10, a large increase in TUNEL-positive cells was seen in the *Ehd4*$^{-/-}$ testis (Fig. 5, panel d and g). The apoptotic cells were presumed to be spermatogonia as well as preleptotene or leptotene spermatocytes based on their location in the tubule and the age of the animal (Fig. 5, panel d). The number of apoptotic cells was comparable between wild type and *Ehd4*$^{-/-}$ mice at d20. Interestingly, a second wave of apoptosis was seen in the *Ehd4*$^{-/-}$ testis at d31 (Fig. 5, panel f and g), while apoptosis was comparable between older wild type and *Ehd4*$^{-/-}$ mice (data not shown).

Deletion of EHD4 leads to altered number of germ cells, but not Sertoli cells

While seminiferous tubule diameter was reduced in *Ehd4*$^{-/-}$ vs. *Ehd4*$^{+/+}$ testes beyond day 20, the tubules were slightly larger in *Ehd4*$^{-/-}$ testes at d10 compared to the *Ehd4*$^{+/+}$ testes (Table 3). It is known that the first wave of spermatogenesis involves coincident increase in apoptosis and mitosis (Rodriguez, *et al.*, 1997;Wang, *et al.*, 1998). As increased apoptosis was observed at d10 *Ehd4*$^{-/-}$ testis, we asked if this was associated with increased mitosis thereby accounting for a larger rather than smaller seminiferous tubule diameter in *Ehd4*$^{-/-}$ testis at day 10. Therefore, we stained testis sections for proliferating cell nuclear antigen (PCNA) which is known to stain spermatogonia and leptotene spermatocytes in d10 mouse testis (Chapman and Wolgemuth, 1994). Interestingly, an increase in PCNA-positive cells was seen in d10 *Ehd4*$^{-/-}$ testis compared to *Ehd4*$^{+/+}$ testis (Fig. 6 panel c). In addition, in d10 *Ehd4*$^{+/+}$ testis, PCNA-positive cells are arranged in the periphery of seminiferous tubules, while a large number of tubules in the *Ehd4*$^{-/-}$ testis had more centrally located PCNA-positive cells which appeared to be preleptotene and leptotene primary spermatocytes (Fig. 6 panel c and d). It is worth noting that many of the PCNA positive cells in the lumen were also positive for TUNEL (data not shown).

Sertoli cells play a significant role in germ cell nutrition and regulation of spermatogeneis. A decrease in Sertoli cell numbers could lead to smaller testes sizes and the germ cell death observed might be an indirect consequence of lower Sertoli cell numbers. As the seminiferous tubule sizes were smaller in the d20 and d31 *Ehd4*$^{-/-}$ testis (Fig. 4), we enumerated Sertoli cells and germ cells in the tubules and compared germ cell to Sertoli cell ratios. While Sertoli cell numbers were comparable between *Ehd4*$^{+/+}$ and *Ehd4*$^{-/-}$ testis at d20, the relative number of germ cells/100 Sertoli cells was lower in the *Ehd4*$^{-/-}$ testis (Table 4). The same trend was seen at d31, though it was difficult to find round tubules at similar stages in both *Ehd4*$^{+/+}$ and *Ehd4*$^{-/-}$ testis and this resulted in analyses of fewer tubules (Supplementary Material, Table 2). Overall, the results described above suggest that deletion of EHD4 does not result in a reduction in Sertoli cell numbers and the reduction in germ cell numbers might be unrelated to Sertoli cell numbers. That being said, the intimate nature of Sertoli cell-germ cell association during spermatogenesis necessitates future studies to address the effect of EHD4 deletion in Sertoli cells.

EHD4 deletion results in head abnormalities in elongated spermatids and dysregulation of the seminiferous epithelium

Although the different cell types (Sertoli cells, spermatogonia, spermatocytes, round and elongated spermatids) were present in the d31 and d75 *Ehd4*$^{-/-}$ testis, closer examination revealed defects in the seminiferous epithelium. In the d31 *Ehd4*$^{+/+}$ testis (Fig. 7a, panel a-d), step 9 spermatids show normal changes in nuclear shape, step 10-11 spermatids show normal acrosome formation and step 14 spermatids show normal shaped nucleus with highly condensed chromatin. In comparison, d31 *Ehd4*$^{-/-}$ testis contain abnormal shaped spermatids, and these are first obvious in step 9-10 spermatids (Fig. 7a, panel e) and they persist in later steps (Fig. 7, panel f-h). At d75, normal spermatogenesis is apparent in *Ehd4* $^{+/+}$ testis with all stages present and tubules that exhibit normal numbers of germ cells and germinal layers (Fig. 7b, panel a-b). In the *Ehd4*$^{-/-}$ testis, the normal arrangement of cell types is lost, indicating dysregulation of the spermatogenic cycle (Fig. 7b, panel c-f). For example, step 16 spermatids were mixed with step 10, and abnormal aggregates of step 16 spermatids were observed (Fig. 7b, panel c) indicating failure of spermiation of some mature sperm. Also, some tubules showed absence of germinal layers; for example, elongated spermatids were absent and pachytene spermatocytes missing in most areas of the tubule shown in Figure 7b, panel d, while step 5-6 round spermatids were observed in normal numbers. Based on the above observations, we conclude that EHD4 is required for normal germ cell numbers at puberty and for proper elongated spermatid development in adult animals.

Reduced epididymal sperm count and subfertility in *Ehd4*$^{-/-}$ males

To analyze the impact of the observed defects in the *Ehd4*$^{-/-}$ testis on sperm production, sperm counts and motility assays were performed on caudal epididymal sperm from adult (d110) *Ehd4*$^{+/+}$ and *Ehd4*$^{-/-}$ mice. As shown in Table 5, a moderate reduction in sperm counts was present in *Ehd4*$^{-/-}$ epididymides when compared to wild type, and they showed comparable motility and forward progression.

Mice with reduced sperm counts can still sire pups and might not show any observable defects in fertility. Since it was possible to maintain *Ehd4*$^{-/-}$ mice as a line, we analyzed litter sizes and litter intervals of breeding pairs of *Ehd4*$^{-/-}$ mice and compared them to wild type mice. As shown in Table 6 there was a slight, but reproducible reduction in fertility seen in *Ehd4*$^{-/-}$ mice, characterized by fewer pups per litter. We have observed copulatory plugs in *Ehd4*$^{-/-}$ females when housed with *Ehd4*$^{-/-}$ males which suggest normal mating behavior. The extent of reduced fertility in *Ehd4*$^{-/-}$ males is further demonstrated by the following experiments: when three 75d *Ehd4*$^{+/+}$ and *Ehd4*$^{-/-}$ males were housed for 15 days with females of corresponding genotypes, all three *Ehd4* wild type females became pregnant and gave birth to pups, while one *Ehd4*-null female did not become pregnant. This female when housed with another *Ehd4* null animal became pregnant and gave birth to pups indicating that the female was reproductively competent. In another experiment, when a single d75 *Ehd4*$^{+/+}$ male was housed with three *Ehd4*$^{+/+}$ females for 15 days, all three females became pregnant and gave birth to pups. However, when a d75 *Ehd4*$^{-/-}$ male was housed with three *Ehd4*$^{-/-}$ females for 15 days, only 2 females became pregnant indicating that *Ehd4*$^{-/-}$ males have slightly reduced fertility. This female subsequently became pregnant and gave birth to pups when housed with a different *Ehd4*$^{-/-}$ male, indicating that the female was reproductively competent.

EHD4 is highly expressed in primary spermatocytes in adult mice

In order to characterize the cell types in the testis that express EHD4, we examined formalin-fixed testis sections from adult male mice by immunohistochemistry using antibodies against EHD4. As shown in Figure 8, EHD4 protein is highly expressed in

primary spermatocytes, especially preleptotene, leptotene and early pachytene spermatocytes in wild type mice. As expected, this staining was absent in *Ehd4*$^{-/-}$ testis. The high levels of EHD4 predominantly in germ cells and not Sertoli cells further support our conclusion that the germ cell death seen in the early testis might be a direct consequence of EHD4 deletion in germ cells.

EHD4 expression peaks during pre-pubertal testis development and is much lower in adult animals

Deletion of EHD4 in the pre-pubertal testis results in a dramatic increase in apoptosis at d10 and notably smaller testis size and seminiferous tubule diameter by d31, yet severe abnormalities are not seen in the seminiferous epithelium in adult mice. Previously, we have observed increased EHD1 protein expression in the cochlea of *Ehd4*$^{-/-}$ mice that may provide functional compensation so that no hearing defects were observed (Sengupta, *et al.*, 2009) in the *Ehd4*$^{-/-}$ mice. Therefore, we speculated that the lack of severe effects of EHD4 deletion on spermatogenesis in the adult mouse may be due to functional compensation by other EHD proteins. However, no clear information is available on EHD protein levels during testis development.

In order to examine the EHD4 protein levels during testis development, we performed Western blotting on whole testis lysates prepared from wild type mice at post-natal d9, d10, d12, d15, d27 and d61. EHD4 protein was detected in testis lysates from all time points, though levels were lower at d61. EHD1 was also detected in all testis lysates; however, EHD1 levels increased several fold after d27 and remained high at d61 (Fig. 9, panel a; more clear in the shorter exposure shown in Fig. 9, panel b). Further analyses using expanded time points more clearly demonstrate that EHD4 is temporally regulated during testis development (Fig. 9, panel c). EHD4 protein levels were barely detectable at d7, and increased almost 2 fold by d10 and remained high at d15. The levels decreased by d31, and were low at d62, and stayed at these low levels until d143. However, EHD1 showed a distinctly different expression pattern with lower levels at d7, d10 and d15, a nearly 10-fold increase by d31 and persistence of these high levels at d143 (Fig. 9, panel c). The pattern of EHD2 expression was similar to EHD4, with lower expression at d7 and increased levels at d10, d15 and d31 and lower levels in adult animals; this is more obvious in panel d (Fig. 9). EHD3 levels were lower before puberty and higher protein levels were observed at d31 and d87. This is the first demonstration of temporal regulation of expression of EHD protein family members during the development of an organ in mammals.

Deletion of EHD4 differentially affects the levels of other EHD proteins in the testis

Since we have previously observed compensation by EHD1 upon EHD4 deletion in the cochlea (Sengupta, *et al.*, 2009), we examined if deletion of EHD4 affects the expression levels of other EHD proteins in the testis. Testes were collected from *Ehd4*$^{+/+}$ and *Ehd4*$^{-/-}$ mice at d7, d31, d62 and d110 and whole testis lysates were analyzed by Western blotting. As expected, EHD4 was expressed in *Ehd4*$^{+/+}$ testis and missing in *Ehd4*$^{-/-}$ testis (Fig. 10). Interestingly, testes of EHD4-null mice showed several alterations in the levels of other EHD proteins. At d7, a reduction in EHD1 levels was observed in EHD4-null testis and this effect was more marked at day 31, while little effect was seen at d110. EHD4 deletion had a distinctly different effect on EHD2 levels: at d7, a reduction in EHD2 protein levels was seen; however, at d31 a significant increase was observed which persisted at d110. We did not see major changes in EHD3 expression following EHD4 deletion (data not shown). Taken together, our results indicate that absence of the EHD4 protein results in a marked change in the expression of other family members that may ameliorate the functional effects of EHD4 deficiency during testis development.

Minor abnormalities were observed in the pancreas of *Ehd4*$^{-/-}$ mice and this is described in detail under Supplementary Material.

Discussion

EHD4 belongs to a highly conserved family of Eps15 homology domain-containing proteins. Cell biological studies demonstrate a critical role for these proteins at various steps in endocytic recycling (George, *et al.*, 2007; Blume, *et al.*, 2007; Naslavsky, *et al.*, 2009; Sharma, *et al.*, 2008). From previous analyses using complementation of the *C. elegans rme-1* mutant with human EHD proteins and studies in mammalian cells, we suggested that EHD proteins might have distinct as well as overlapping functions. Another study comparing all four EHD proteins suggested that each EHD protein might be restricted to certain tissues and/or intracellular compartments, where they might perform distinct functions (Blume, *et al.*, 2007). In order to clearly identify the roles of EHD proteins in mammalian physiology, we have begun to engineer their deficiencies in mice. Here, we report the generation and initial characterization of *Ehd4* knockout mice. Targeted deletion of the first exon completely abrogated the expression of EHD4; no truncated product initiating from internal translation initiation sites were observed in organs of the *Ehd4*$^{-/-}$ mice as analyzed by Western Blotting, indicating that the targeting strategy was successful.

Interestingly, several organs showed moderate elevation in the levels of other EHD proteins. *Ehd4*$^{+/+}$, *Ehd4*$^{+/-}$ and *Ehd4*$^{-/-}$ mice were born at expected Mendelian ratios (Table 1), had comparable body weights, showed no developmental or growth defects, and exhibited normal viability. Even though *Ehd4*$^{-/-}$ mice did not show any defects in viability, they exhibited a severe reduction in testis size to approximately half the wild type size (Fig.3). On closer examination, *Ehd4*$^{-/-}$ mice showed a slight reduction in testis weights at d10, which became more pronounced at d20, was almost 50% of wild type by d31 and remained reduced throughout the life of the animal. We found evidence for increased early germ cell proliferation and apoptosis, the latter increasing at later developmental stages (Fig.5, 6). Coupled with spatially-irregular PCNA-positive cells in developing seminiferous tubules of EHD4-null mice, these findings indicate that the balance of survival and apoptotic stimuli that tightly regulate germ cell development is upset in *Ehd4*$^{-/-}$ testis. Our results strongly suggest that the reduction in germ cell numbers contribute to the striking difference in testis size and seminiferous tubule diameter in the pre-pubertal period.

We show that EHD4 is expressed in preleptotene, leptotene and early pachytene spermatocytes in the adult testis (Fig. 8) and this agrees well with the increase in EHD4 protein levels at d10 and d15, time points at which these cell types first appear in the developing testis (Fig. 9). Deletion of EHD4 in the adult testis results in head abnormalities in elongated spermatids and clumping of step 16 spermatids (Fig. 7b). It is presumable that the subsequent phagocytosis of abnormal spermatids by Sertoli cells could eventually lead to a decrease in post-meiotic germ cells and contribute to reduced testis sizes and tubule diameters in adult *Ehd4*$^{-/-}$ testis.

We did not find a significant alteration in Sertoli cell numbers per tubule (Table 4, Supplementary Material Table 2). However, germ cell to Sertoli cell ratio was markedly reduced at d20 and d31, co-incident with a reduction in tubule diameter and testis size (Table 4). While these initial results suggests a primarily germ cell defect in EHD4-null mice, given the intimate cross-talk and complex interactions between Sertoli and germ cells for normal spermatogenesis, a Sertoli cell involvement in the phenotypes observed cannot be ruled out until mice with Sertoli cell and germ cell specific deletion of EHD4 are analyzed.

How might deletion of the endocytic recycling regulator, EHD4, cause aberrant proliferation and apoptosis in the pre-pubertal testis? It is well known that spermatogonia depend on several paracrine factors including growth factors produced by Sertoli cells which bind to receptors on germ cells and elicit signaling to promote survival, differentiation or self-renewal of germ cells. For example, glial cell-derived neurotrophic factor (GDNF) produced by Sertoli cells regulates self renewal and differentiation of mouse spermatogonial stem cells (SSCs) (Meng, *et al.*, 2000) by binding to RET receptors and a ligand specific co-receptor, GFRalpha. Signaling as a result of ligand binding to the receptor is essential for proliferation of spermatogonial stem cells (SSCs), while deletion of GDNF/GFR alpha signaling triggers differentiation of SSCs (He, *et al.*, 2007). Apoptotic pathway in germ cells also involves signaling through ligand-activated receptors that are endocytosed. For example, Fas ligand produced by Sertoli cells induces aopotosis of germ cells through death receptor Fas (Lee, *et al.*, 1997). Up regulation of Fas in spermatocytes is known to be important for their apoptosis in the first wave of spermatogenesis (Lizama, *et al.*, 2007). Therefore, it is quite conceivable that inhibition or aberrant functioning of endocytic pathways in the absence of EHD4 could alter cell surface levels of critical receptors involved in proliferation and apoptosis and thus upset the balance of proliferative versus apoptotic signaling resulting in increased death of germ cells.

Why does EHD4 deletion elicit a rather dramatic effect in the pre-pubertal testis without causing severe fertility defects in adult mice? A proper assessment of defects due to the deletion of EHD4 needs to take into account expression of other EHD proteins, since previous work suggests that EHD proteins can hetero-oligomerize and a compensatory increase in EHD1 levels upon EHD4 deletion has been previously observed in the cochlea (Sengupta, *et al.*, 2009). Since no information was available on the regulation of EHD protein expression in the testis, we analyzed testis from mice encompassing the neonatal, pubertal and sexually mature stages of life. These analyses demonstrate that the expression of multiple EHD proteins is temporally regulated during testis development. For example, EHD1 levels are low in the neonatal and pre-pubertal period, however a spurt in EHD1 expression occurs close to puberty and high levels of EHD1 are present in the adult testis. This large increase in EHD1 levels likely coincide with the appearance of elongated spermatids. Not surprisingly, normal elongated spermatids are absent in *Ehd1*$^{-/-}$ testis and these animals exhibit small testis and are infertile (Rainey MA, *et al*, submitted). Hence, EHD1, not EHD4, might be important for maintenance of spermatogenesis in adult mice, while EHD4 is relatively highly expressed in the pre-pubertal period and apparently functionally critical at this stage than in the adulthood.

It is also noteworthy that deletion of EHD4 alters the pattern of expression of other family members and this likely modulates the functional deficits we observe. The neonatal *Ehd4*$^{-/-}$ testis (d7) shows a decrease in the levels of EHD1 and EHD2 (Fig. 10). Therefore, at d7, depletion of EHD4 effectively results in the functional diminution of three out of four EHD proteins expressed at this time. This is consistent with marked histological perturbations such as increased proliferation and apoptosis seen at d10 in *Ehd4*$^{-/-}$ testis. Closer to puberty (as evidenced from the d31 lysates; Fig. 10), *Ehd4*$^{-/-}$ testis exhibit a reduction in EHD1 and an increase in EHD2 levels. Despite this compensatory increase in EHD2 levels, marked apoptosis is seen at d31 in the *Ehd4*$^{-/-}$ testis. At sexual maturity and beyond (d62 and d110 lysates, Fig. 10), EHD1 levels are high despite deletion of EHD4. Given the dramatic effects of EHD1 deficiency on spermatogenesis (Rainey MA, *et al*, submitted), we therefore suggest that EHD1 (and possibly other expressed EHD proteins) compensate for EHD4 deficiency in adulthood and thereby prevent the development of severe spermatogenesis defects in the adult testis. EHD3 is the only EHD family member whose expression is relatively unaffected by EHD4 deletion. Not surprisingly, our initial analysis of *Ehd*3

knockout mice indicates that deletion of EHD3 does not affect testis size or fertility (data not shown).

Our analyses of EHD protein expression during testis development suggest that EHD proteins function co-operatively in the testis. The compensatory changes in other EHD protein levels upon deletion of EHD4 strongly suggest that levels of EHD proteins are precisely regulated and changes in levels of individual family members affect the levels of other family members potentially at the level of transcription and/or through post-transcriptional mechanisms. Regardless of how this regulation occurs, these dynamic changes are in strong contrast to rather distinct effects of individual EHD gene knock-downs in cultured tumor cell lines that have been reported. Our results suggest that under physiological conditions EHD proteins do not act in isolation and that the function of multiple EHD proteins may contribute to functional outputs either by compensating for each other or based on the necessity to form functional hetero-oligomeric complexes. Indeed, structural studies on EHD2 suggest the possibility that EHD proteins may function as oligomers (Daumke, *et al.*, 2007).

As we have generated *Ehd4*$^{-/-}$ mice (as well as other *Ehd* knockout mice, currently being characterized in our laboratory) employing a conditional gene knockout strategy using floxed alleles, generation of double, triple and quadruple EHD knockout mice and their careful and detailed analysis should help dissect out the specific roles of this evolutionarily conserved family of endocytic regulatory proteins in testis development and function.

In conclusion, we have generated *Ehd4*$^{-/-}$ mice with complete deletion of EHD4 protein expression. While *Ehd4*$^{-/-}$ mice are viable and do not show substantial morbidity or organ abnormalities, male EHD4-null mice exhibit a dramatically reduced testis size beginning at puberty, disturbances in spermatogenesis, moderately reduced sperm counts and a slight reduction in fertility. The results presented here suggest that EHD protein-dependent endocytic recycling may play important roles in the development and maintenance of testis size and function.

Methods

Generation of *Ehd4* gene-targeted mice

A conditional gene knockout targeting vector was generated using the “recombineering” method (Liu, *et al.*, 2003) (plasmids and bacterial strains provided by Dr. Neal G. Copeland, NCI, Frederick, Maryland). In brief, the NCBI Mouse Clone Finder was used to identify likely mouse *Ehd4* gene BAC clones and these were obtained from the Children’s Hospital Oakland Research Institute repository. PCR analysis showed the clone RPCI-23-383I16 (derived from female C57BL/6J mouse tissues) containing the *Ehd4* gene to be most suitable for further manipulations.

Using a series of “recombineering” reactions, an approximately 14 kb DNA fragment containing the first coding exon of *Ehd4* was retrieved into a plasmid and two *loxP* sites flanking this exon were introduced. A *FRT-Neo-FRT* selection cassette immediately preceding the second *loxP* site confers G418 resistance in transfected ES cells, with *FRT* sequences allowing removal of the cassette using FLP DNA recombinase; a single *FRT* and *loxP* sequence remained, keeping gene locus alterations to a minimum. PCR primer sequences used to generate the targeting vector and probes for Southern hybridization are available upon request. A *Not*I-linearized targeting vector was electroporated into the albino B6 strain-derived ES cell line B6T and Southern hybridization using 5′ and 3′ external probes identified 3 out of 96 G418- and gancyclovir-selected clones to be correctly targeted;

these were used to produce chimeric mice by blastocyst injection. One chimera achieved germline transmission of the targeted *Ehd4* allele.

To generate *Ehd4*$^{-/-}$ mice, heterozygous *Ehd4*-targeted mice were mated with B6.FVB-Tg (EIIa-Cre) C5379Lmgd/J mice which express Cre recombinase from the adenovirus EIIa promoter for recombination in a wide range of tissues, including germ cells for transmission of the gene alteration to progeny. Heterozygous *Ehd4*-targeted, *cre* transgene-positive mice were crossed to C57BL/6J (wild-type) mice to generate heterozygous *Ehd4*-deleted, *cre* transgene-negative (*Ehd4*$^{+/-}$) mice, which were used to produce *Ehd4*$^{-/-}$ mice. In addition, heterozygous *Ehd4*-targeted mice were intercrossed to generate homozygous (*Ehd4*$^{fl/fl}$) mice. All mice used in this study have been maintained on the C57BL/6J background.

Breeding and maintenance of mice colonies

Inter-gender crosses of *Ehd4*$^{+/-}$ mice were used to generate *Ehd4*$^{+/+}$ *Ehd4*$^{+/-}$ and *Ehd4*$^{-/-}$ mice. Animals were genotyped by tail PCR and ink-tattooed on toes for identification. Primer sequences used for genotyping *Ehd4* mice are available upon request. All experiments involving animals were approved by the Institutional Animal Care and Use Committee. All animals were treated humanely in accordance with institutional guidelines and that of the National Institutes of Health (NIH) Guide for the Care and Use of Laboratory Animals.

For estimation of litter size and interval, 2 month old male and female mice of the specified genotype were housed together. Cages (n=4 per genotype) were observed, births recorded and litter sizes and litter intervals for each genotype was calculated.

Harvesting of tissues and Western blotting

For Western blots, mice were euthanized using CO_2, organs were removed, washed briefly in PBS and lysed in lysis buffer as described previously (George, *et al.*, 2007). 100 μg aliquots of lysate proteins were separated using 8.5% SDS-PAGE and Western blotted using anti-EHD antibodies described previously. The antibody used to detect EHD4 is raised against CSHRKSLPKAD peptide in EH domain and has been previously shown to be specific to EHD4 (George, *et al.*, 2007).

Immunostaining

Five μm testis cross sections sections from d10, d20, d31 *Ehd4*$^{+/+}$ and *Ehd4*$^{-/-}$mice, were deparaffinized in xylene and rehydrated in graded ethanols followed by PBS. For antigen retrieval, the slides were boiled twice for 10 min in citrate-based antigen unmasking solution (Vector Laboratories, Burlingame, CA, #H-3300) in a microwave. Endogenous peroxidase was inactivated by a 15 min incubation in 3% hydrogen peroxide (Sigma-Aldrich, St. Louis, MO) in PBS. Staining was carried out using the Zymed Laboratories Histostain-SP Kit (Broad Spectrum, DAB, Invitrogen, Carlsbad, CA, #95-9643). PCNA antibody (PC10,Sc-56, Santa Cruz) was used at a 1:50 dilution in PBS/5% fetal bovine serum. For EHD4 staining, formalin fixed 5 μm testes sections from d75 *Ehd4*$^{+/+}$ and *Ehd4*$^{-/-}$mice were deparaffinized as above and boiled as described. The polyclonal rabbit-anti-EHD4 primary antibodies were used at a 1:50 dilution in PBS/5% fetal bovine serum and a goat anti-rabbit Alexa Fluor 488 secondary antibody was used at 1:200 dilution in PBS. The slides were mounted in Vectashield containing DAPI. Confocal images were acquired with a LSM510 fluorescence confocal microscope (Carl Zeiss, Thornwood, NY) under a 40X objective.

Counting of cell types and measurement of seminiferous tubule diameter in the testis

Sequential paraffin-embedded sections were cut and stained using PAS and spermatogenic epithelial cell types were counted on PAS stained testis sections. Different cell types were identified based on the changes of acrosome and nuclear morphology of younger generation spermatids. PCNA stained sections were used to for counting when it was difficult to clearly stage the tubules in the *Ehd4*$^{-/-}$ mice. For measurement of seminiferous tubule diameter, images of the testis sections were acquired using a 10X or 4X objective and all tubules (n=>160) in a section were measured using the "line measure" option in the NIS elements software and tubule numbers in the d75 testis section were counted manually.

TUNEL assay

For TUNEL assay, 5 μm Bouin's fixed testis cross sections from d10, d20 and d31 *Ehd4*$^{+/+}$ and *Ehd4*$^{-/-}$ mice testis were deparaffinized as described. Following antigen retrieval, an In Situ Cell Death Detection kit, POD (Roche) was used for TUNEL and it was performed following the manufacturer's instructions. Appropriate negative and positive controls were included in each experiment. Confocal images of TUNEL were acquired with a LSM510 fluorescence confocal microscope (Carl Zeiss, Thornwood, NY) under either a 10X or 20X objective. TUNEL positive cells were counted from 8 sections (2 sections/testis, 2 testes/mice 2 mice/time point) and plotted.

Sperm count and motility assays

Four *Ehd4*$^{+/+}$ and *Ehd4*$^{-/-}$ male mice (d110) housed with females for 15 days were euthanized, and testes were spleen weighed. The cauda epididymides were carefully dissected into 0.9 ml of pre-warmed DMEM and samples were then incubated for 20 min at 37°C, 10 μl of the diluted sperm suspension was analyzed using a Meckler's counting chamber. At least 3 independent measurements were made for each sample. All sperm that moved were considered motile, while sperm that crossed the field were counted for forward progression.

Supplementary Material

Refer to Web version on PubMed Central for supplementary material.

Acknowledgments

We thank Laura Willoughby for help with genotyping and members of the Band Laboratories for helpful suggestions and discussion.

This work was supported by: the NIH Grants CA105489, CA99163, CA87986, CA116552 and CA99900, to H.B., and CA94143, CA96844 and CA81076 to V.B.; DOD Breast Cancer Research Grants DAMD17-02-1-0303 (H.B.), DAMD17-02-1-0508 (V.B.), W81XWH-05-1-0231 (V.B.), W81XWH-07-1-0351 (V.B.) and W81XWH-08-1-0612 (M.G.); Avon Breast Cancer Fund, Northwestern University; and the Jean Ruggles-Romoser Chair of Cancer Research (H.B.) and the Duckworth Family Chair of Breast Cancer Research (VB). MN acknowledges support from ENH Research Career Development Award. MR acknowledges support from Grant T32 CA70085 from the National Institutes of Health to the Robert H. Lurie Comprehensive Cancer Center Training Program in Signal Transduction and Cancer.

Literature Cited

Bellve AR, Cavicchia JC, Millette CF, O'Brien DA, Bhatnagar YM, Dym M. Spermatogenic cells of the prepuberal mouse. isolation and morphological characterization. J Cell Biol 1977;74:68–85. [PubMed: 874003]

Blume JJ, Halbach A, Behrendt D, Paulsson M, Plomann M. EHD proteins are associated with tubular and vesicular compartments and interact with specific phospholipids. Exp Cell Res 2007;313:219–231. [PubMed: 17097635]

Braun A, Pinyol R, Dahlhaus R, Koch D, Fonarev P, Grant BD, Kessels MM, Qualmann B. EHD proteins associate with syndapin I and II and such interactions play a crucial role in endosomal recycling. Mol Biol Cell 2005;16:3642–3658. [PubMed: 15930129]

Chapman DL, Wolgemuth DJ. Expression of proliferating cell nuclear antigen in the mouse germ line and surrounding somatic cells suggests both proliferation-dependent and -independent modes of function. Int J Dev Biol 1994;38:491–497. [PubMed: 7848832]

Clermont Y. Kinetics of spermatogenesis in mammals: Seminiferous epithelium cycle and spermatogonial renewal. Physiol Rev 1972;52:198–236. [PubMed: 4621362]

Daumke O, Lundmark R, Vallis Y, Martens S, Butler PJ, McMahon HT. Architectural and mechanistic insights into an EHD ATPase involved in membrane remodelling. Nature 2007;449:923–927. [PubMed: 17914359]

Doherty KR, Demonbreun AR, Wallace GQ, Cave A, Posey AD, Heretis K, Pytel P, McNally EM. The endocytic recycling protein EHD2 interacts with myoferlin to regulate myoblast fusion. J Biol Chem 2008;283:20252–20260. [PubMed: 18502764]

George M, Ying G, Rainey MA, Solomon A, Parikh PT, Gao Q, Band V, Band H. Shared as well as distinct roles of EHD proteins revealed by biochemical and functional comparisons in mammalian cells and C. elegans. BMC Cell Biol 2007;8:3. [PubMed: 17233914]

Grant BD, Caplan S. Mechanisms of EHD/RME-1 protein function in endocytic transport. Traffic. 2008

Guilherme A, Soriano NA, Furcinitti PS, Czech MP. Role of EHD1 and EHBP1 in perinuclear sorting and insulin-regulated GLUT4 recycling in 3T3-L1 adipocytes. J Biol Chem 2004;279:40062–40075. [PubMed: 15247266]

He Z, Jiang J, Hofmann MC, Dym M. Gfra1 silencing in mouse spermatogonial stem cells results in their differentiation via the inactivation of RET tyrosine kinase. Biol Reprod 2007;77:723–733. [PubMed: 17625109]

Jovic M, Naslavsky N, Rapaport D, Horowitz M, Caplan S. EHD1 regulates beta1 integrin endosomal transport: Effects on focal adhesions, cell spreading and migration. J Cell Sci 2007;120:802–814. [PubMed: 17284518]

Kuo HJ, Tran NT, Clary SA, Morris NP, Glanville RW. Characterization of EHD4, an EH domain-containing protein expressed in the extracellular matrix. J Biol Chem 2001;276:43103–43110. [PubMed: 11533061]

Lee DW, Zhao X, Scarselletta S, Schweinsberg PJ, Eisenberg E, Grant BD, Greene LE. ATP binding regulates oligomerization and endosome association of RME-1 family proteins. J Biol Chem 2005;280:17213–17220. [PubMed: 15710626]

Lee J, Richburg JH, Younkin SC, Boekelheide K. The fas system is a key regulator of germ cell apoptosis in the testis. Endocrinology 1997;138:2081–2088. [PubMed: 9112408]

Liu P, Jenkins NA, Copeland NG. A highly efficient recombineering-based method for generating conditional knockout mutations. Genome Res 2003;13:476–484. [PubMed: 12618378]

Lizama C, Alfaro I, Reyes JG, Moreno RD. Up-regulation of CD95 (apo-1/Fas) is associated with spermatocyte apoptosis during the first round of spermatogenesis in the rat. Apoptosis 2007;12:499–512. [PubMed: 17195944]

Maxfield FR, McGraw TE. Endocytic recycling. Nat Rev Mol Cell Biol 2004;5:121–132. [PubMed: 15040445]

Meng X, Lindahl M, Hyvonen ME, Parvinen M, de Rooij DG, Hess MW, Raatikainen-Ahokas A, Sainio K, Rauvala H, Lakso M, Pichel JG, Westphal H, Saarma M, Sariola H. Regulation of cell fate decision of undifferentiated spermatogonia by GDNF. Science 2000;287:1489–1493. [PubMed: 10688798]

Naslavsky N, McKenzie J, Altan-Bonnet N, Sheff D, Caplan S. EHD3 regulates early-endosome-to-golgi transport and preserves golgi morphology. J Cell Sci 2009;122:389–400. [PubMed: 19139087]

Naslavsky N, Rahajeng J, Chenavas S, Sorgen PL, Caplan S. EHD1 and Eps15 interact with phosphatidylinositols via their Eps15 homology domains. J Biol Chem 2007a;282:16612–16622. [PubMed: 17412695]

Naslavsky N, Rahajeng J, Rapaport D, Horowitz M, Caplan S. EHD1 regulates cholesterol homeostasis and lipid droplet storage. Biochem Biophys Res Commun 2007b;357:792–799. [PubMed: 17451652]

Naslavsky N, Rahajeng J, Sharma M, Jovic M, Caplan S. Interactions between EHD proteins and Rab11-FIP2: A role for EHD3 in early endosomal transport. Mol Biol Cell 2006;17:163–177. [PubMed: 16251358]

Print CG, Loveland KL. Germ cell suicide: New insights into apoptosis during spermatogenesis. Bioessays 2000;22:423–430. [PubMed: 10797482]

Rapaport D, Auerbach W, Naslavsky N, Pasmanik-Chor M, Galperin E, Fein A, Caplan S, Joyner AL, Horowitz M. Recycling to the plasma membrane is delayed in EHD1 knockout mice. Traffic 2006;7:52–60. [PubMed: 16445686]

Rodriguez I, Ody C, Araki K, Garcia I, Vassalli P. An early and massive wave of germinal cell apoptosis is required for the development of functional spermatogenesis. EMBO J 1997;16:2262–2270. [PubMed: 9171341]

Sengupta S, George M, Miller KK, Naik K, Chou J, Cheatham MA, Dallos P, Naramura M, Band H, Zheng J. EHD4 and CDH23 are interacting partners in cochlear hair cells. J Biol Chem 2009;284:20121–20129. [PubMed: 19487694]

Shao Y, Akmentin W, Toledo-Aral JJ, Rosenbaum J, Valdez G, Cabot JB, Hilbush BS, Halegoua S. Pincher, a pinocytic chaperone for nerve growth factor/TrkA signaling endosomes. J Cell Biol 2002;157:679–691. [PubMed: 12011113]

Sharma M, Naslavsky N, Caplan S. A role for EHD4 in the regulation of early endosomal transport. Traffic 2008;9:995–1018. [PubMed: 18331452]

Valdez G, Akmentin W, Philippidou P, Kuruvilla R, Ginty DD, Halegoua S. Pincher-mediated macroendocytosis underlies retrograde signaling by neurotrophin receptors. J Neurosci 2005;25:5236–5247. [PubMed: 15917464]

Wang RA, Nakane PK, Koji T. Autonomous cell death of mouse male germ cells during fetal and postnatal period. Biol Reprod 1998;58:1250–1256. [PubMed: 9603260]

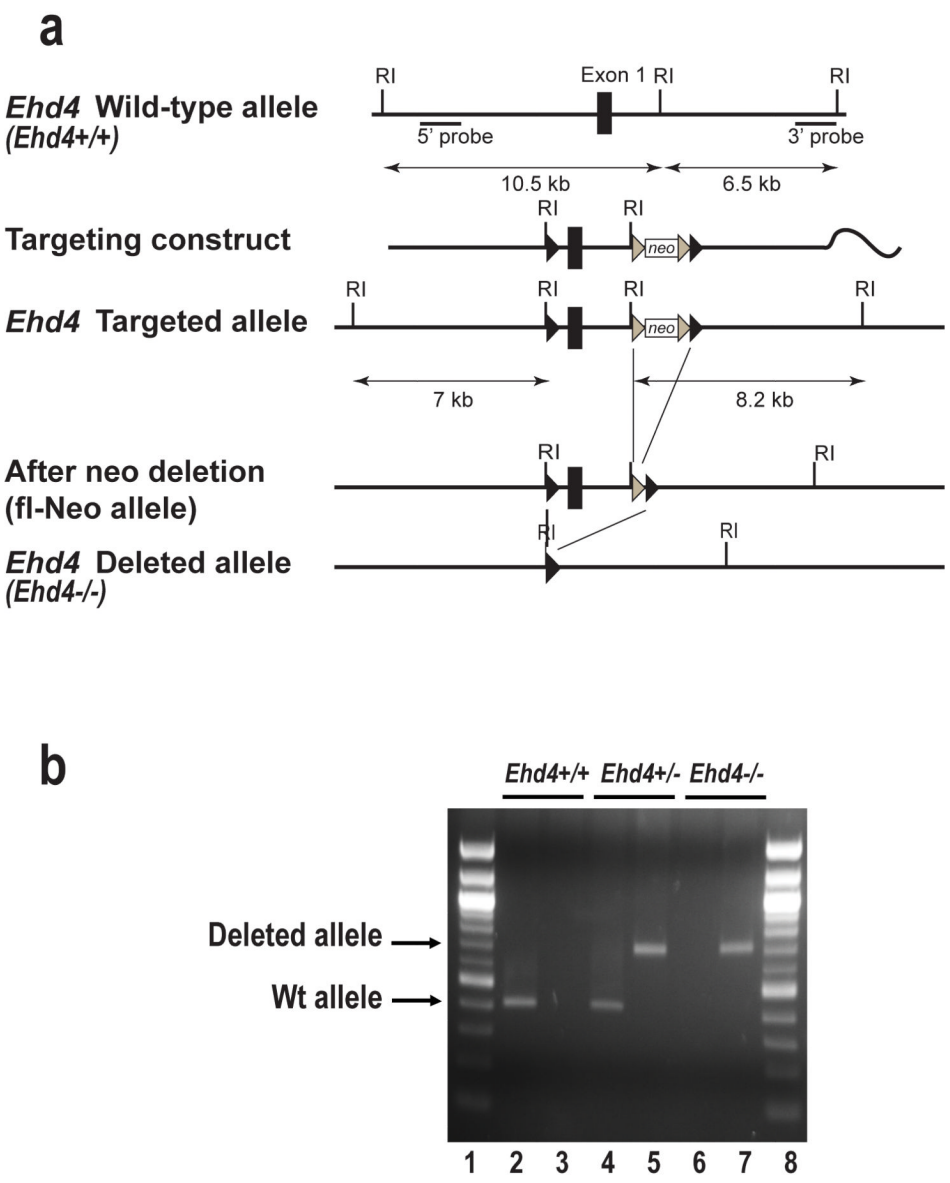

FIG. 1. Generation of *Ehd4*$^{-/-}$ mice using Cre/*loxP*-mediated genetic recombineering

(a) Partial restriction map of the murine *Ehd4* locus, the targeting vector and the mutated *Ehd4* loci. The first exon was flanked by *loxP* sequences for deletion by Cre/*loxP*-mediated recombination. Black rectangles represent exons, black and grey triangles represent *loxP* and *FRT* sequences, respectively. RI, *Eco*RI. (b) Genotyping tail DNA by PCR. Each DNA sample was subjected to PCR using two primer pairs to amplify the wild type allele (404 bp; lanes 2, 4 and 6) and the deleted allele (687 bp; lanes 3, 5 and 7), respectively, and agarose gel electrophoresis was used. Wt, wild type.

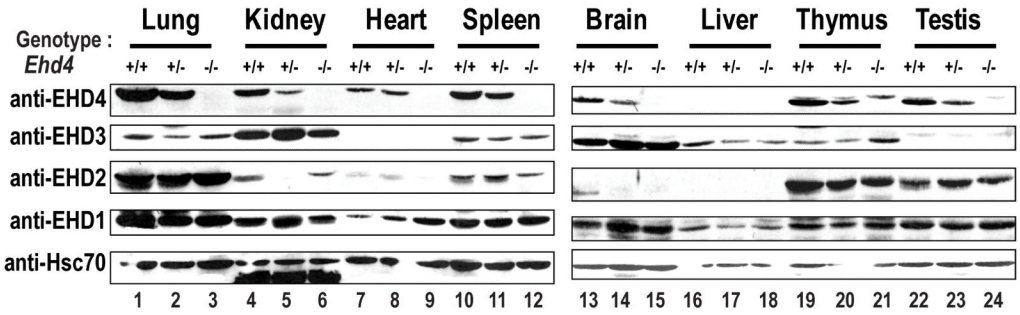

FIG. 2. EHD protein expression in *Ehd4*$^{+/+}$, *Ehd4*$^{+/-}$ and *Ehd4*$^{-/-}$ mouse organs

Lysates of the indicated organs were prepared from 40-day old male mice as described in Methods. 100 μg aliquots of tissue lysates were separated on 8.5% SDS-PAGE gels followed by serial Western blotting using the indicated anti-EHD antibodies (in the following order: EHD4, EHD3, EHD2 and EHD1) and anti-Hsc70 antibodies. Shadow bands in lanes 1, 2, 10 and 11 (beneath EHD2) are bleed through of the EHD4 band from the previous probing. The higher band in the *Ehd4*$^{-/-}$ thymus (lanes 19-21) is probably a non-specific band. Hsc70 served as a loading control; multiple bands likely represent tissue specific isoforms.

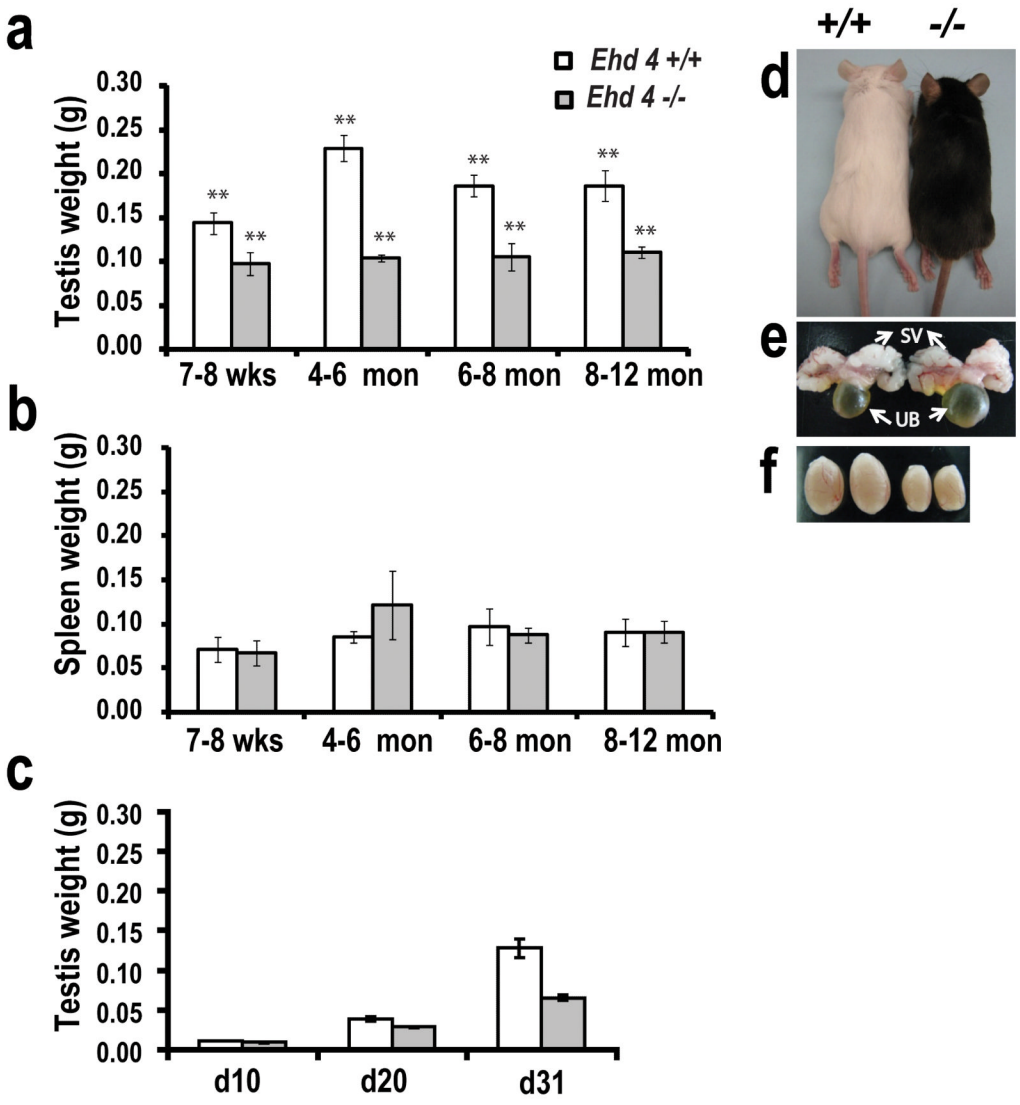

FIG. 3. Reduced testicular size in *Ehd4*$^{-/-}$ mice

(a) Testis and (b) spleens were obtained from *Ehd4*$^{+/+}$ and *Ehd4*$^{-/-}$ mice ranging in age from 7 weeks (wks) to 12 months (mon), weighed (n ≥ 3) and plotted against age. (c) Testis from *Ehd4*$^{+/+}$ and *Ehd4*$^{-/-}$ mice (n=3) at post-natal day 10 (d10), d20 and d31 were weighed and plotted against age. Open and grey bars indicate *Ehd4*$^{+/+}$ and *Ehd4*$^{-/-}$ mouse organs, respectively. (** indicates $p<0.05$ using two-tailed analysis). (d-f) Two 5-month old mice and their (e) seminal vesicles (SV), urinary bladder (UB) and (f) testis are shown. The *Ehd4*$^{+/+}$ mouse pictured has white coat color because the ES cells are derived from an Albino B6 mouse.

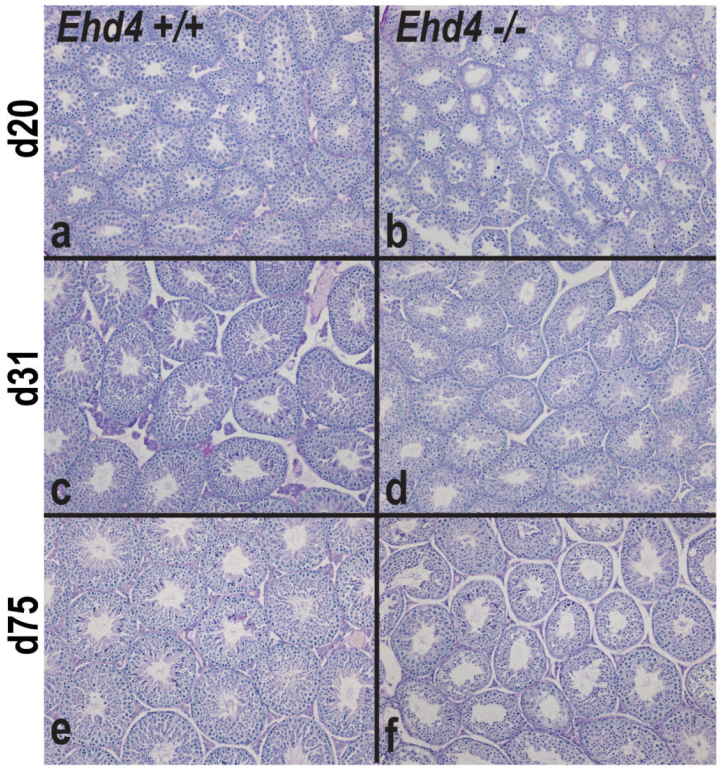

FIG. 4. Loss of EHD4 leads to a progressive reduction of seminiferous tubule diameter with increasing age

Ehd4$^{+/+}$ and *Ehd4*$^{-/-}$ mice (n=3) at post natal d10, d20 and d31 were euthanized, their testis dissected from the scrotal sac, immersion-fixed and PAS-stained as described in Methods. Images were acquired using a 20X objective. Panels a, c and e represent testis sections from *Ehd4*$^{+/+}$ mice at d20, d31 and d75 respectively, while panels b, d, f represent testis sections from *Ehd4*$^{-/-}$ mice at d20, d31 and d75 respectively.

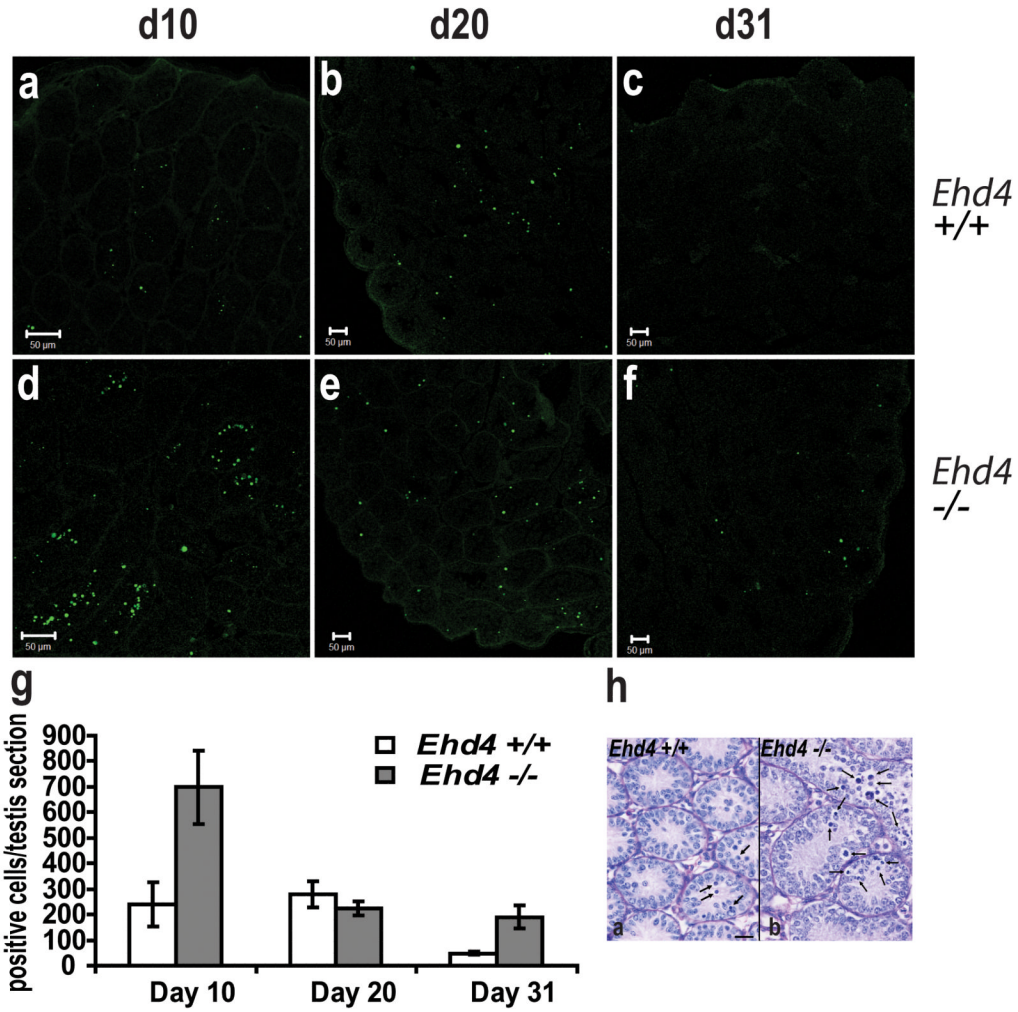

FIG. 5. Deletion of EHD4 leads to an increase in apoptosis at d10 and d31 in *Ehd4*$^{-/-}$ testis

Testis sections from d10, d20 and d31 *Ehd4*$^{+/+}$ and *Ehd4*$^{-/-}$ male mice were subjected to TUNEL assay as described in Methods. Panels a-c represent confocal images from d10, d20 and d31 *Ehd4*$^{+/+}$ testis, respectively, while panels d-f represent confocal images from d10, d20 and d31 *Ehd4*$^{-/-}$ testis, respectively. Images covering the entire testis section were acquired for 8 testis sections per time point and (g) apoptotic nuclei were counted. (h) 40X objective images of PAS-stained d10 testis from *Ehd4*$^{+/+}$ and *Ehd4*$^{-/-}$ mice. Arrows point to apoptotic bodies. Bar =20 µm.

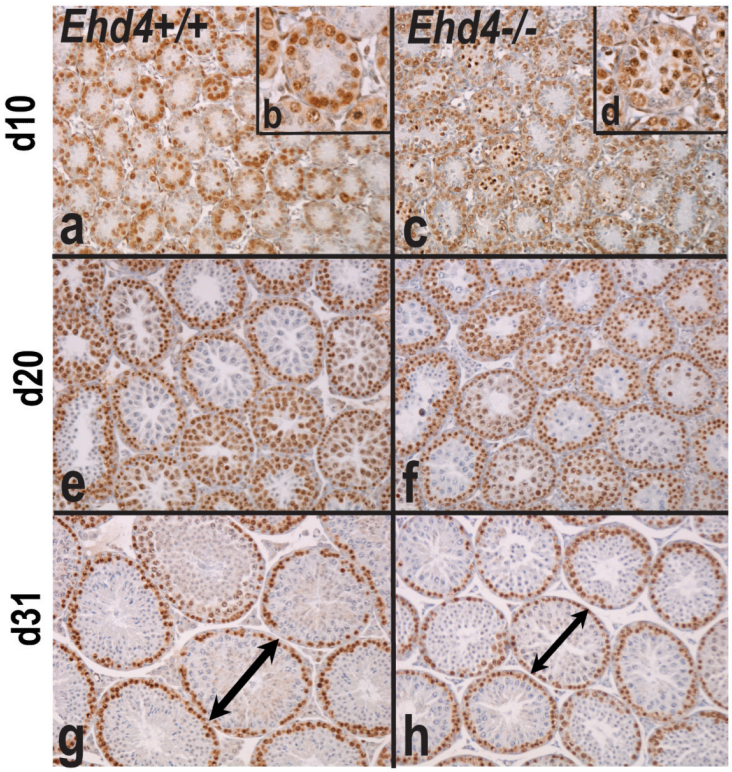

FIG. 6. Deletion of EHD4 leads to an increase in PCNA-positive cells at d10

Testis sections from d10, d20 and d31 *Ehd4*$^{+/+}$ and *Ehd4*$^{-/-}$ male mice were subjected to PCNA staining as described in Methods. Panel a, e, and g represent 20X objective light microscope images of PCNA staining from d10, d20 and d31 *Ehd4*$^{+/+}$ testis, respectively, while panels c, f and h represent images from d10, d20 and d31 *Ehd4*$^{-/-}$ testis, respectively. Insets b and d represent 40X objective light microscope images. The seminiferous tubule diameter is indicated using the two-headed arrows in panels g and h.

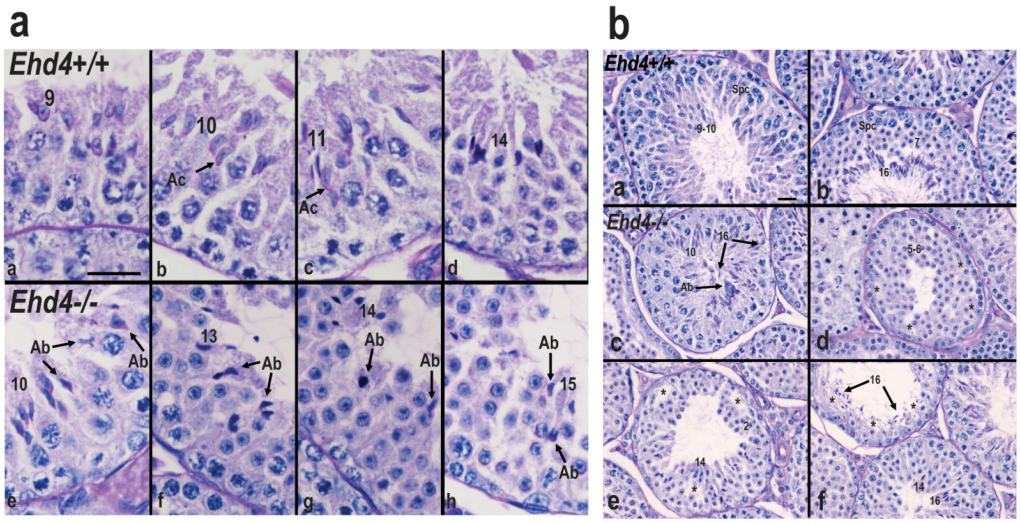

FIG. 7. EHD4 deletion results in head abnormalities in elongated spermatids and dysregulation of the seminiferous epithelium

PAS-stained testis sections from d31 *Ehd4*$^{+/+}$ mice (7a, panels a-d) mice show acrosome (Ac) formation in 9, 10-11 and step 14 spermatids. *Ehd4*$^{-/-}$ testis (7a, panels e-h) show abnormal (Ab) spermatid formation in steps 9-10 spermatids, abnormal spermatids were also noted in later steps (13-15). Testis sections from d75 *Ehd4*$^{+/+}$ mice (7b, panels a-b) show normal spermatogenesis with all stages present, normal numbers of germ cells and normal appearance of the germinal layers. Spc=spermatocyte; 7, 9-10,16=spermatids. In *Ehd4*$^{-/-}$ testis (7b, panels c-f), step 16 spermatids were mixed with step 10 spermatids. Abnormal (Ab) aggregates of step 16 spermatids were also observed. (d) Missing germinal layers with step 5-6 round spermatids observed in normal numbers, pachytene spermatocytes missing in most areas of the tubule (*) and elongated spermatids absent. (e) Missing pachytene spermatocytes (*) and step 2 round spermatids and step 14 elongated spermatids were greatly reduced in number. (f) One seminiferous tubule is missing round spermatids and pachytene spermatocytes (*) and a few step 16 spermatids remain after failure of spermiation. In the adjacent tubule, steps 14 and 16 elongated spermatids are present together in Stage II, indicating failure of spermiation in the prior cycle of the epithelium. Bar=20 μm.

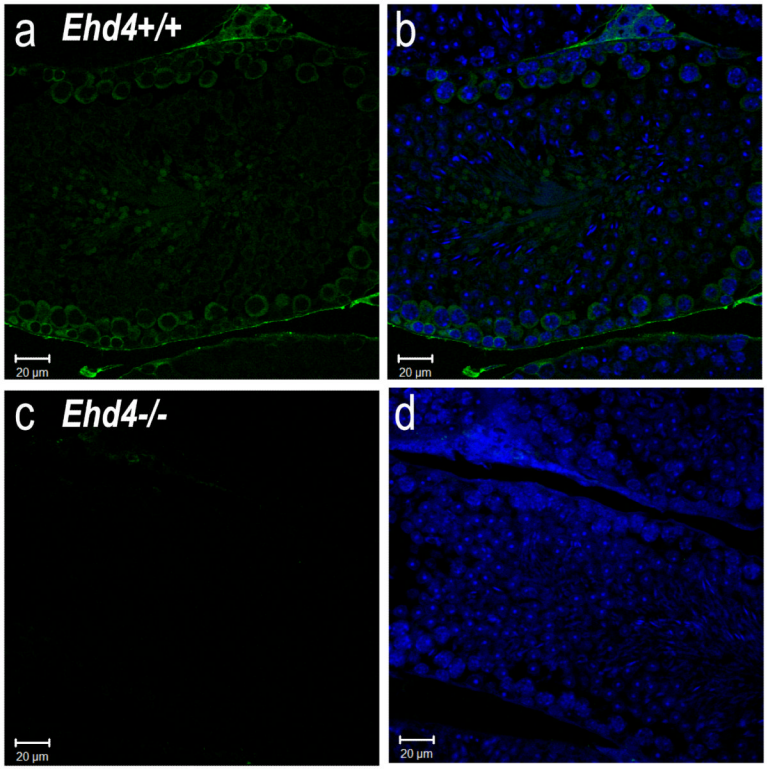

FIG. 8. EHD4 is highly expressed in primary spermatocytes in adult mice

Testes sections from *Ehd4*$^{+/+}$ (a,b) and *Ehd4*$^{-/-}$ (c,d) adult mice were immersion-fixed and immunostained for EHD4 as described in Methods and examined by confocal microscopy. (a) Positive staining near the basement membrane indicates EHD4 protein (green) is present in primary spermatocytes in *Ehd4*$^{+/+}$ mice; lower levels can be seen in other cell types in the testis. (c) EHD4 staining was absent in *Ehd4*$^{-/-}$ testis. (b,d) DAPI staining (blue) highlights the nuclei of all cells in the seminiferous epithelia.

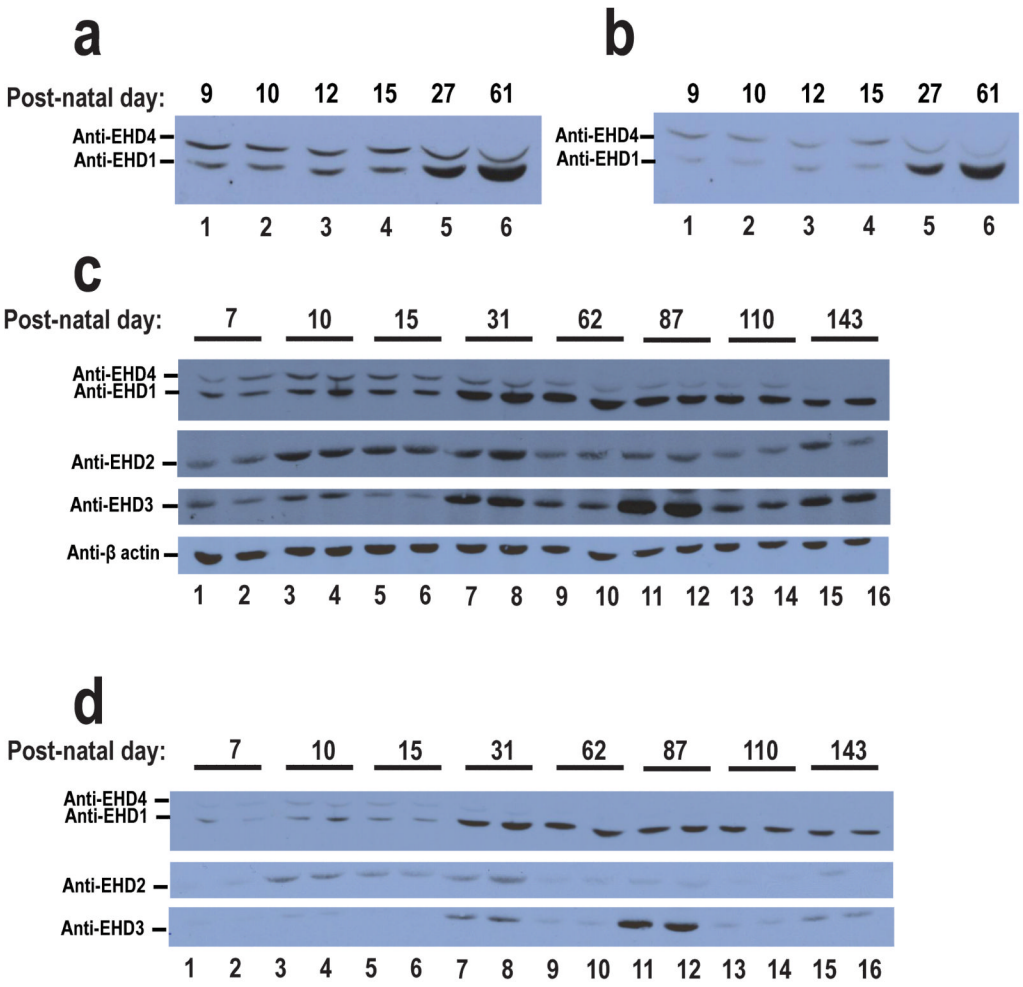

FIG. 9. EHD4 expression peaks during pre-pubertal testis development and is much lower in adult animals

Testicular lysates were prepared from (a,b) 9-61 and (c,d) 7-143 day old *Ehd4*$^{+/+}$ male mice as described in Methods. (c,d) Two different mouse testis lysates are shown for each age. 50 μg aliquots of tissue lysates were separated on 8% SDS-PAGE gels. Western blots were performed using the indicated anti-EHD antibodies and anti-β-actin antibodies as a loading control. (a,c) Long exposures and (b,d) short exposures are shown.

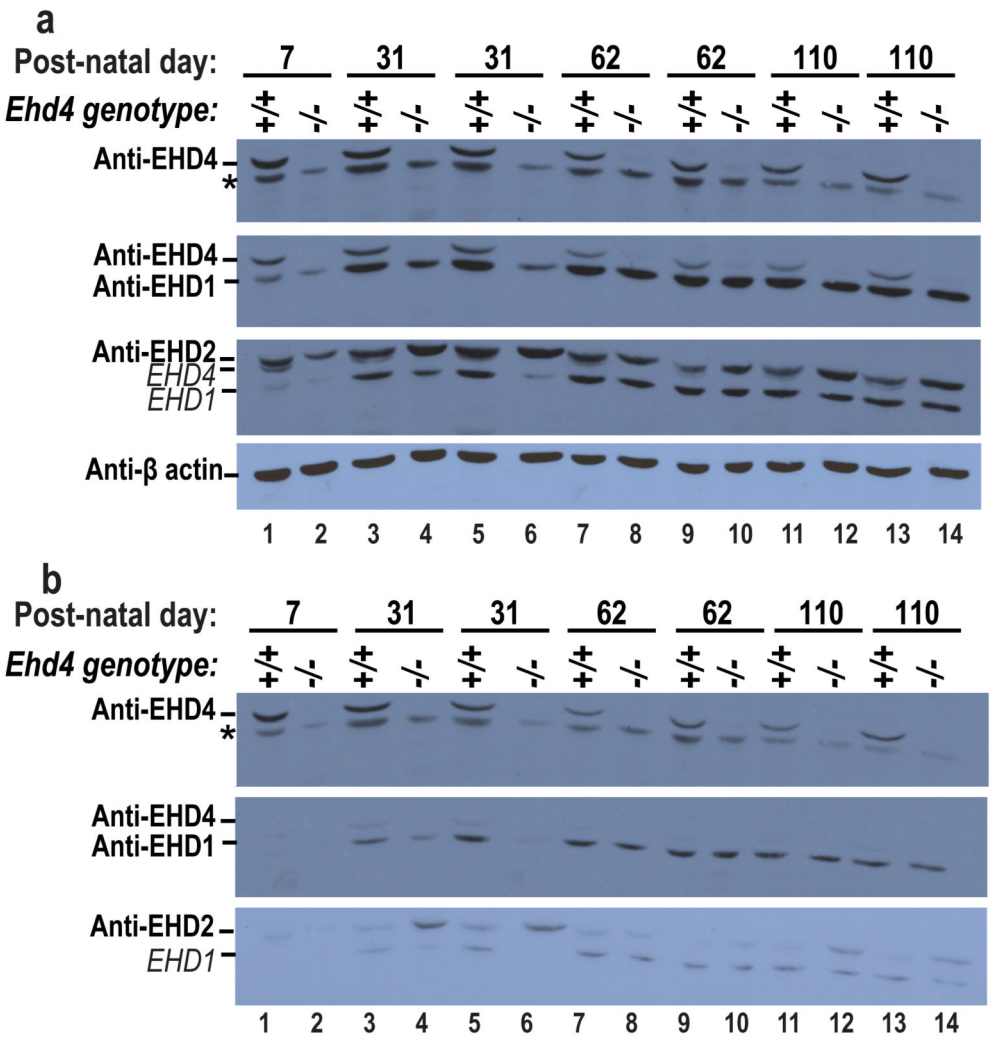

FIG. 10. Deletion of EHD4 differentially affects the levels of other EHD proteins in the testis

Testicular lysates were prepared from 7-110 day old *Ehd4*$^{+/+}$ and *Ehd4*$^{-/-}$ male mice as described in Methods. 50 μg aliquots of tissue lysates were separated on 8% SDS-PAGE gels. Western blots were performed using the indicated anti-EHD antibodies and anti-β-actin antibodies as a loading control. Serial blots were performed in the following order: EHD4, EHD1 followed by EHD2. (a) Long exposures and (b) short exposures are shown. * - non-specific band. *EHD4* and *EHD1* represent bleed through from the previous blots.

Table 1

Genotypes of pups from *Ehd4*$^{+/-}$ intercrosses

	Female	Male	*Ehd4*$^{+/+}$ pups	*Ehd4*$^{+/-}$ pups	*Ehd4*$^{-/-}$ pups	Total
n=7	*Ehd4* $^{+/-}$	*Ehd4* $^{+/-}$	48 (24%)	100 (51%)	49 (25%)	197

n values denote the number of breeding pairs, some breeding pairs produced multiple litters.% was calculated as genotype per total pups.

Table 2

Body weights of *Ehd4*$^{+/+}$ and *Ehd4*$^{-/-}$ mice

Males	***Ehd4*$^{+/+}$**	***Ehd4*$^{-/-}$**
< 8 weeks	19.6 ± 0.5 g (n = 3)	17.9 ± 0.4 g (n = 8)
9-23 weeks	29.7 ± 3.5 g (n =9)	26.7 ± 2.9 g (n =20)

Females	***Ehd4*$^{+/+}$**	***Ehd4*$^{-/-}$**
< 8 weeks	13.9 ± 3.0 g (n = 3)	14.4 ± 2.3 g (n = 3)
9-23 weeks	20.9 ± 1.2 g (n = 9)	19.3 ± 3.4 g (n=15)

n values denote the number of animals weighed in each category.

Table 3

Diameter of seminiferous tubules in *Ehd4*$^{+/+}$ and *Ehd4*$^{-/-}$ testis

Age	Genotype	Diameter of seminiferous tubule (μm) (n =300)
d10	*Ehd4* $^{+/+}$	105 ± 24
d10	*Ehd4* $^{-/-}$	120 ± 21
d20	*Ehd4* $^{+/+}$	111 ± 25
d20	*Ehd4* $^{-/-}$	98 ± 20
d31	*Ehd4* $^{+/+}$	163 ± 23
d31	*Ehd4* $^{-/-}$	129 ± 19
d75	*Ehd4* $^{+/+}$	186 ± 22
d75	*Ehd4* $^{-/-}$	138 ± 22

n denotes the minimum number of tubules measured.

Table 4

Cell numbers in the *Ehd4*$^{+/+}$ and *Ehd4*$^{-/-}$ testis

Genotype	*Ehd4*$^{+/+}$	*Ehd4*$^{-/-}$
Sertoli cells/tubule	14 ± 3	12 ± 3
Total Sertoli cells	378	346
PCNA + spermatogonia	8 ± 3	5 ± 2
PCNA + spermatocyte	64 ± 10	60 ± 9
Total spermatogonia	210	147
PCNA − spermatocyte	30 ± 8	21 ± 7
Total spermatocyte	1786	1673
Total round spermatid	151	52
No. of spermatids/100 Sertoli cells	30	12
No. of spermatocytes/100 Sertoli cells	381	367

n=20 circular tubules were counted in 2 sections from 2 mice per genotype

Table 5

Sperm count and motility in *Ehd4*$^{+/+}$ and *Ehd4*$^{-/-}$ mice

Genotype	*Ehd4*$^{+/+}$ (n=4)	*Ehd4*$^{-/-}$ (n=4)
Sperm count (10^6/ml)	58.2 ± 4.5	14.3 ± 4.3
Motility (%)	44.5 ± 14.6	44.7 ± 8.8
Forward progression (%)	79.3 ± 5.4	70.7 ±5.8

n= number of animals aged 110 days used for sperm analysis

Table 6

Litter size and litter interval in *Ehd4*$^{+/+}$ intercrosses and *Ehd4*$^{-/-}$ intercrosses

	***Ehd4*$^{+/+}$ (n=8)**	***Ehd4*$^{-/-}$ (n=8)**
Litter size	5.5	5.4*
Litter interval	25 days	29 days*

n= number of litters analyzed

* indicates that p>0.05 using two-tailed analysis (not statistically significant)